THE JOURNAL OF BIOLOGICAL CHEMISTRY VOL. 282, NO. 46, pp. 33583–33592, November 16, 2007

Regulation of Insulin Secretion by SIRT4, a Mitochondrial ADP-ribosyltransferase*[S]

Received for publication, July 5, 2007, and in revised form, August 20, 2007 Published, JBC Papers in Press, August 22, 2007, DOI 10.1074/jbc.M705488200

Nidhi Ahuja[‡1], Bjoern Schwer[‡1], Stefania Carobbio[§1], David Waltregny[¶1], Brian J. North[‡], Vincenzo Castronovo[¶], Pierre Maechler[§], and Eric Verdin[‡2]

From the [‡]Gladstone Institute of Virology and Immunology, University of California, San Francisco, California 94158, [§]Department of Cell Physiology and Metabolism, University Medical Center, University of Geneva, CH-1211 Geneva 4, Switzerland, [¶]Metastasis Research Laboratory, University of Liege, B-4000 Liege, Belgium

Sirtuins are homologues of the yeast transcriptional repressor Sir2p and are conserved from bacteria to humans. We report that human SIRT4 is localized to the mitochondria. SIRT4 is a matrix protein and becomes cleaved at amino acid 28 after import into mitochondria. Mass spectrometry analysis of proteins that coimmunoprecipitate with SIRT4 identified insulin-degrading enzyme and the ADP/ATP carrier proteins, ANT2 and ANT3. SIRT4 exhibits no histone deacetylase activity but functions as an efficient ADP-ribosyltransferase on histones and bovine serum albumin. SIRT4 is expressed in islets of Langerhans and colocalizes with insulin-expressing β cells. Depletion of SIRT4 from insulin-producing INS-1E cells results in increased insulin secretion in response to glucose. These observations define a new role for mitochondrial SIRT4 in the regulation of insulin secretion.

Histone deacetylases are enzymes that catalyze the removal of acetyl groups from the ϵ-amino group of lysine residues and are separated into three classes. Sirtuins, the class III histone deacetylases, are homologous to the yeast transcriptional repressor, Sir2p, and are NAD^+-dependent enzymes (1–3). Seven sirtuins have been identified in the human genome (4, 5). They share a conserved Sir2 catalytic core domain and exhibit variable amino- and carboxyl-terminal extensions that contribute to their unique subcellular localization and may also regulate their catalytic activity.

The subcellular distribution, substrate specificity, and cellular functions of sirtuins are quite diverse (reviewed in Refs. 1–3). SIRT1 is found in the nucleus, where it functions as a transcriptional repressor via histone deacetylation. SIRT1 can also regulate transcription by modifying the acetylation levels of transcription factors, such as MyoD, FOXO, p53, and NF-κB (6–12). The SIRT2 protein is found in the cytoplasm, where it associates with microtubules and deacetylates lysine 40 of α-tubulin (13). The SIRT3 protein is localized in the mitochondrial matrix (14, 15), where it is proteolytically processed at its NH_2 terminus, yielding a mature protein that has protein deacetylase activity (14). These observations indicate that the targets of sirtuins are not restricted to histone proteins but extend to acetylated proteins in other subcellular compartments.

Sirtuins also differ in their substrate specificities. For instance, SIRT1, -2, and -3 have robust activity on chemically acetylated histone H4 peptides, whereas SIRT5 has weak but detectable activity, and SIRT4, -6, and -7 have no detectable activity on the same substrate (13). Interestingly, a sirtuin from *Archaeoglobus fulgidus*, Sir2-Af1, which has close homology with SIRT5, also has weak activity on a histone peptide but significantly stronger activity on an acetylated bovine serum albumin substrate (16, 17). Similarly, both SIRT1 and SIRT2 can deacetylate p53; however, only SIRT2 deacetylates lysine 40 of α-tubulin (13, 17).

Recently, SIRT6 was demonstrated to be a nuclear ADP-ribosyltransferase (18), whereas a *T. brucei* SIR2 homologue exhibited both histone NAD-dependent ADP-ribosyltransferase and deacetylase activities (19). These observations indicate that sirtuins can function either as NAD-dependent protein deacetylases or as ribosyltransferases.

The substrate specificities of SIRT3 to -7 are unknown. Determining the localization patterns of these proteins is the first step in elucidating the physiologically relevant targets for deacetylation by each of these enzymes. Here, we report that SIRT4 is targeted to the mitochondrial matrix, where it interacts with insulin-degrading enzyme and the ADP/ATP carrier protein. Depletion of SIRT4 from insulin producing INS-1E cells results in increase in secretion of insulin from these cells in response to glucose, suggesting that SIRT4 negatively regulates insulin secretion in these cells.

EXPERIMENTAL PROCEDURES

Tissue Culture—HEK293, HEK293T and HeLa cells were grown in Dulbecco's modified Eagle's medium (Invitrogen) supplemented with 10% fetal bovine serum (Gemini Bio-products, Woodland, CA) in the presence of penicillin, streptomycin, and 2 mM L-glutamine (Invitrogen). The clonal β cell line INS-1E (20), derived from parental INS-1 cells (21), was grown

* This work was supported by funds from the J. David Gladstone Institutes (to E. V.), the Sandler Foundation at the University of California, San Francisco (to E. V.), the Ellison Medical Foundation (to E. V.), and the Swiss National Science Foundation (to P. M.). The UCSF Biomolecular Resource Center Mass Spectrometry facility was supported by a grant from the Sandler New Technology Fund. The costs of publication of this article were defrayed in part by the payment of page charges. This article must therefore be hereby marked "*advertisement*" in accordance with 18 U.S.C. Section 1734 solely to indicate this fact.

[S] The on-line version of this article (available at http://www.jbc.org) contains supplemental figures.

[1] These authors contributed equally to this work.

[2] A Senior Scholar in Aging of the Ellison Medical Foundation. To whom correspondence should be addressed: Gladstone Institute of Virology and Immunology/UCSF, 1650 Owens St., San Francisco, CA 94158. Tel.: 415-734-4808; Fax: 415-355-0855; E-mail: everdin@gladstone.ucsf.edu.

in Roswell Park Memorial Institute 1640 medium supplemented with 5% fetal calf serum, 10 mM Hepes, 2 mM glutamine, 100 units/ml penicillin, 100 μg/ml streptomycin, 1 mM sodium pyruvate, and 50 μM 2-mercaptoethanol. Adherent cultures of INS-1E cells were transfected with control siRNA[3] or siRNA against SIRT4 (synthesized by Dharmacon Inc., Chicago, IL) and further cultured in complete RPMI 1640 medium for 3 days before experiments.

Plasmids and Mutagenesis—The human *SIRT4* gene was cloned in a derivative of pcDNA3.1(+) (FLAG vector) to generate the construct encoding SIRT4-FLAG, as described (13). Deletion mutants of SIRT4 were constructed by using oligo-directed, PCR-based mutagenesis. The QuikChange site-directed mutagenesis kit (Stratagene, La Jolla, CA) was used for site-directed mutagenesis.

Antibodies—The following antibodies were obtained commercially: anti-Hsp60 (clone 4B9/89; Affinity Bioreagents, Golden, CO), anti-Hsp70 (clone JG1; Affinity Bioreagents), anti-Hsp90 (SPS-771; Stressgen Biotechnologies, San Diego, CA), anti-cytochrome *c* oxidase subunit IV (clone 20E8-C12; Molecular Probes, Inc., Eugene, OR), anti-cytochrome *c* (clone 7H8.2C12; Pharmingen, San Diego, CA), anti-FLAG M2 (Sigma), anti-insulin-degrading enzyme (clone BC-2; Covance, Berkeley, CA), Cy2-conjugated anti-mouse secondary antibody (Jackson ImmunoResearch Laboratories, West Grove, PA), and rabbit polyclonal anti-FLAG (Sigma). SIRT4 antiserum was raised in rabbits (Sigma-Genosys) against a COOH-terminal peptide corresponding to the last 15 amino acids of SIRT4 (NH_2-LNSRCGELLPLIDPC-COOH). ANT2-specific antiserum was kindly provided by Dr. Douglas C. Wallace (University of California, Irvine) and immune affinity-purified as described (22).

Immunofluorescence and Confocal Microscopy—HeLa cells grown on glass coverslips were transfected with Lipofectamine (Invitrogen). After 24 h of transfection, the cells were washed with phosphate-buffered saline (PBS) and incubated with Dulbecco's modified Eagle's medium containing 40 nM Mito-Tracker Red (CMXRos; Molecular Probes) for 45 min at 37 °C, washed in PBS, and incubated with Dulbecco's modified Eagle's medium for 1 h. The cells were then washed, fixed in 3.7% paraformaldehyde for 10 min at 37 °C, permeabilized with 0.2% Triton X-100 for 10 min, and blocked with 1% bovine serum albumin for 10 min. Immunostaining was then done with monoclonal anti-FLAG M2 antibody (1:500) for 1 h followed by incubation with a Cy2-conjugated anti-mouse secondary antibody (1:500) for 30 min. The cells were washed twice with PBS containing 0.1% Tween 20 and once briefly with water. The coverslips were mounted on glass slides and analyzed by confocal laser-scanning microscopy with an Olympus BX60 microscope equipped with a Radiance 2000 confocal setup (Bio-Rad).

Differential Centrifugation—HEK293T cells were harvested by centrifugation and resuspended in ice-cold buffer A (250 mM sucrose, 10 mM KCl, 1.5 mM $MgCl_2$, 1 mM EDTA, 1 mM EGTA, 1 mM dithiothreitol, 20 mM HEPES-KOH, pH 7.5) containing protease inhibitor mixture (Complete; Roche Applied Science). Cells were homogenized using Dounce homogenization (Wheaton, Millville, NJ). After removal of nuclei and unbroken cells by centrifugation at 770 × *g* for 10 min, the heavy membrane (HM) fraction was prepared by centrifugation at 5,500 × *g* for 10 min. The resulting supernatant was centrifuged at 100,000 × *g* for 1 h to separate the light membrane (LM) fraction (pellet) from the cytosolic proteins (S100). The HM and the LM fractions were solubilized in lysis buffer (50 mM Tris-HCl, pH 7.5, 0.5 mM EDTA, 0.5% Nonidet P-40, 150 mM NaCl), and the protein content was determined with Bio-Rad DC protein assay reagent. Equal amounts of protein from each fraction were subjected to SDS-PAGE and analyzed by immunoblotting.

Transient Transfections and Immunoprecipitations—HEK293T cells were transfected by the calcium phosphate DNA precipitation method and harvested 48 h after transfection. Mitochondria were isolated by differential centrifugation as described above and lysed in lysis buffer (50 mM Tris-HCl, pH 7.5, 0.5 mM EDTA, 0.5% Nonidet P-40, 150 mM NaCl) in the presence of a protease inhibitor mixture. SIRT4-FLAG was immunoprecipitated with anti-FLAG M2-agarose affinity gel (Sigma) for 2 h at 4 °C from total cell lysate. Immunoprecipitated material was washed three times for 15 min each with lysis buffer and dissolved in SDS-PAGE sample buffer.

Protease Accessibility Assays—Mitochondria from HEK293T cells were resuspended in SM buffer (250 mM sucrose, 10 mM MOPS-KOH, pH 7.2) and aliquoted in three tubes. Mitochondria were pelleted by centrifugation and resuspended in SM buffer, hypotonic buffer (10 mM MOPS-KOH, pH 7.2), or SM buffer containing 1% (w/v) Triton X-100. The mitochondria were incubated on ice for 5 min and digested with Proteinase K (150 μg/ml) on ice for 15 min. Proteolysis was stopped with 2 mM phenylmethylsulfonyl fluoride, and proteins were precipitated in 15% trichloroacetic acid, collected by centrifugation, washed with acetone, recentrifuged, and analyzed by immunoblotting.

Alkaline Extraction Experiments—Mitochondria were isolated from HEK293T cells expressing SIRT4-FLAG and resuspended in freshly prepared ice-cold 0.1 M sodium carbonate (pH 11.5) for 30 min at 4 °C. Mitochondria were centrifuged at 100,000 × *g* for 30 min at 4 °C followed by solubilization in SDS sample buffer. Supernatant proteins were concentrated by trichloroacetate precipitation, solubilized in SDS sample buffer, and analyzed by immunoblotting.

Mitochondrial Sonication—Mitochondria were isolated from cells expressing SIRT4-FLAG, resuspended in sonication buffer (20 mM Tris, pH 7.5, 100 mM NaCl), and sonicated with a microtip sonicator (Cole-Parmer Instruments, model CP130, three times for 6 s, 40% duty cycle, microtip output setting 6). The sonicated sample was centrifuged at 100,000 × *g* for 30 min at 4 °C to separate the membranes (pellet) from the soluble proteins.

In Vitro ADP-ribosylation—HEK293 cells overexpressing SIRT4-FLAG were solubilized in lysis buffer (50 mM Tris-HCl, pH 7.5, 0.5 mM EDTA, 0.5% Nonidet P-40, 150 mM NaCl) in the presence of a protease inhibitor mixture, and SIRT4-FLAG was immunoprecipitated with anti-FLAG M2-agarose affinity gel

[3] The abbreviations used are: siRNA, small interfering RNA; IDE, insulin-degrading enzyme; BSA, bovine serum albumin; PBS, phosphate-buffered saline; HM, heavy membrane; LM, light membrane; MOPS, 4-morpholinepropanesulfonic acid; MALDI-TOF, matrix-assisted laser desorption ionization time-of-flight.

(Sigma) for 2 h at 4 °C from total cell lysate. Immunoprecipitated material was washed three times for 15 min each with lysis buffer containing 300 mM NaCl and followed by SIRT4-FLAG elution with 100 μg/ml FLAG peptide (Sigma). The ADP-ribosylation reaction contained 10 μg of BSA (Sigma) or total histone proteins (Roche Applied Science) and the following buffer: 10 mM dithiothreitol, 2 mM EDTA, and 50 mM Tris-HCl (pH 8.0). The reaction was initiated by adding 2.5 μCi of [^{32}P]NAD and SIRT4 (0.5 μg/reaction), and the reaction was allowed to proceed for 1 h at 37 °C. Free radioactivity was removed from the samples using spin column (Amersham Biosciences). Samples were mixed with SDS-PAGE loading buffer and separated on 12% SDS-polyacrylamide gels after boiling for 5 min. The gels were dried, and autoradiography was performed.

Generation of Stable Cell Line Overexpressing SIRT4-FLAG and SIRT5-FLAG—SIRT4 (or SIRT5)-FLAG-pcDNA3.1+ vector or empty-pcDNA3.1+ control vector was linearized with the enzyme SspI, gel-purified, and transfected into HEK293 cells. After 48 h of transfection, the cells were selected in medium containing 700 μg/ml G418.

SIRT4 Immunoprecipitation and Peptide Mass Fingerprinting—Cells expressing SIRT4-FLAG were harvested and solubilized in lysis buffer (50 mM Tris-HCl, pH 7.5, 0.5 mM EDTA, 0.5% Nonidet P-40, 150 mM NaCl) in the presence of a protease inhibitor mixture, and SIRT4-FLAG was immunoprecipitated with anti-FLAG M2-agarose affinity gel (Sigma) overnight at 4 °C from total cell lysate. Immunoprecipitated material was washed three times for 15 min each with lysis buffer containing 300 mM NaCl and resuspended in SDS-sample buffer. The samples were subjected to SDS-PAGE followed by Coomassie Blue staining. Bands corresponding to proteins specifically interacting with SIRT4 were excised and prepared for mass spectrometry. Gel slices were destained in 25 mM ammonium bicarbonate, 50% acetonitrile. Gel pieces were treated with 100% acetonitrile until shrinking of the gel pieces was noted. Acetonitrile was removed, and the gel pieces were dried in a vacuum centrifuge. Samples were reduced by treatment with 10 mM dithiothreitol solution for 45 min at 56 °C. The supernatant was removed, and the samples were alkylated in 55 mM iodoacetamide solution for 30 min in darkness at room temperature. After washing in 25 mM ammonium bicarbonate for 15 min, the gel pieces were treated with 100% acetonitrile for 5 min and completely dried in a vacuum centrifuge. 25 μl of trypsin (12.5 ng/ml) were added to the dried gel pieces, followed by incubation on ice for 30 min. 25 mM ammonium bicarbonate was added to cover the gel pieces. After in-gel digestion for 16 h at 37 °C, the supernatant was transferred to a fresh tube, and peptides were extracted twice by vortexing the gel pieces for 20 min in 50% acetonitrile, 5% trifluoroacetic acid. Aqueous and organic peptide extracts were combined and concentrated under vacuum. Peptide mass fingerprints were obtained by mixing 0.5 μl of each in-gel digest peptide extract with 0.5 μl of matrix solution (α-cyano-4-hydroxycinnamic acid (5 mg/ml) in 50% acetonitrile, 50% water, 0.1% trifluoroacetic acid) directly on a stainless steel target. After co-crystallization of the peptide mixture with the matrix, peptide mass maps were obtained using a Voyager DE STR MALDI-TOF mass spectrometer (Applied Biosystems). In the MALDI-TOF process, peptides were ionized following a matrix-analyte crystal irradiation with a pulsed nitrogen laser (337 nm) that struck the sample at a frequency of 20 Hz. A voltage of 25 kV accelerated the peptide ions out of the ion source into the flight tube after a 125-ns delay. Monoprotonated peptide ions were temporally separated according to their mass/charge ratios as they drifted down the flight tube through the reflector mass analyzer, eventually striking the detector. Individual peptide masses were determined by measuring the time it took each ion to travel the distance from its origin to the detector. Delayed extraction of peptide ions from the ion source in combination with the kinetic energy-focusing properties of the reflector (also called the ion mirror) provided mass resolution sufficient for determining the monoisotopic mass of each peptide. Close proximity external calibration enabled peptide masses to be measured within +50–100 ppm of their theoretical values. Protein identification was accomplished by comparing the experimentally generated set of peptide masses with theoretically predicted sets of tryptic peptides derived from each protein in the Swiss-Prot data base (available on the World Wide Web) by a process of "*in silico* digestion." Data base searches were performed using the Aldente Peptide Mass Fingerprinting Tool available to the public on the World Wide Web.

Immunoprecipitations and Western Blotting—HEK293 cells stably expressing SIRT4-FLAG, SIRT5-FLAG, or a FLAG-control vector were plated in 100-mm dishes. Confluent cells were rinsed off with ice-cold PBS, washed twice in PBS, and lysed in lysis buffer (1% Nonidet P-40, 1 mM EDTA, 150 mM NaCl, 50 mM Tris, pH 7.4) containing protease inhibitors (Roche Applied Science EDTA-free mixture) for 1 h on ice. Lysates were cleared (16,100 × *g*, 15 min, 4 °C) and immunoprecipitated with anti-FLAG M2-agarose (Sigma) for 3 h at 4 °C. Immunoprecipitates were washed five times with lysis buffer and analyzed by Western blotting.

Immunohistochemistry—Detection of SIRT4 protein in human tissues was performed on normal human tissue samples using the immunoperoxidase technique and the ABC Vectastain Elite kit (Vector Laboratories, Inc., Burlingame, CA). An anti-human SIRT4 antibody raised against a synthetic peptide composed of amino acids 240–254 (DKVDFVHKRVKEADS) of human SIRT4 was used (Orbigen, San Diego, CA). Five-μm-thick sections of formalin-fixed paraffin-embedded tissue were deparaffinized in xylene and rehydrated in graded alcohols. After blocking of endogenous peroxidase activity with 1.5% hydrogen peroxide in methanol for 30 min, the sections were incubated with 1% normal goat serum in PBS for 60 min. Rabbit anti-SIRT4 antibody (1:150 dilution) was incubated overnight at 4 °C, followed by biotinylated goat anti-rabbit IgG antibody and the avidin-biotin-peroxidase complex. Washes were performed three times with PBS after each incubation step. Peroxidase activity was developed by a solution of 3,3′-diaminobenzidine tetrahydrochloride (Vel, Leuven, Belgium) dissolved in PBS and 0.03% H_2O_2. The 3,3′-diaminobenzidine tetrahydrochloride solution was filtered and applied to the sections for 3 min. Carazzi's hematoxylin was used to counterstain the slides followed by dehydration and mounting. Control experiments were performed with omission of the first antibody in the immunoperoxidase assay. Detection of insulin expression by

the β cells of the pancreatic islets of Langerhans was performed on serial sections of normal human pancreas using the ABC Vectastain Elite kit and a mouse monoclonal anti-insulin antibody at a dilution of 1:500 (clone 2D11-H5; Santa Cruz Biotechnology, Inc., Santa Cruz, CA). Other controls included normal rabbit IgGs (purchased from Serotec, purified polyclonal rabbit IgG from normal rabbit serum) and rabbit anti-bone sialoprotein antibody (LF-83, provided by L. W. Fisher, National Institutes of Health) on normal human pancreas or on a case of poorly differentiated human prostate cancer. Photomicrographs of the slides were taken with a Zeiss microscope equipped with a Leica camera.

siRNA Preparation—siRNAs corresponding to the *SIRT4* gene were designed as recommended and were chemically synthesized by Dharmacon RNA Technologies (Dharmacon Inc., Chicago, IL).

Transfections—Transfection of control siRNA, siRNA against SIRT4 for down-regulation, pFLAG-control, and pFLAG-SIRT4 cDNA for up-regulation were all performed using Lipofectamine 2000 (Invitrogen) in 24-well plates according to the manufacturer's specifications. Briefly, 2×10^5 INS-1E cells were seeded per well into 24-well plates, reaching 50–60% confluence the day of transfection. siRNAs mixtures were incubated for 30 min with Lipofectamine 2000 diluted in serum-free RPMI 1640 before transfer to cells. Next, cells were treated with the respective mixtures for 6 h in the incubator before medium replacement. Transfected cells were kept in culture for 3 days before proceeding to experiments. Different siRNA-SIRT4 concentrations (250, 500, and 1000 nM) were tested in INS-1E cells, and efficiency was assessed by quantitative real time PCR. Overexpression was carried out using 0.14 μg of SIRT4 plasmid DNA/well.

Quantitative Real Time PCR—INS-1E cells cultured in 24-well plates were transfected with siRNA-SIRT4. Three days after transfection, total RNA was extracted using the RNeasy Mini Kit (Qiagen), and 2 μg was converted into cDNA. Primers for rat SIRT4 and rat cyclophilin were designed using the Primer Express Software (Applera Europe). Real time PCR was performed using an ABI 7000 sequence detection system (Applera Europe), and PCR products were quantified fluorometrically using the SYBR Green core reagent kit. The values obtained were normalized to the values of rat cyclophilin mRNA. Rat SIRT4 primers were as follows: 5′-CCA TCC AGC ACA TTG ATT TCA-3′; 5′-GGC CAG CCC ACA AAG TTT C-3′. Rat cyclophilin primers were as follows: 5′-TCA CCA TCT CCG ACT GTG GA-3′; 5′-AAA TGC CCG CAA GTC AAA GA-3′.

Immunoblotting—Ten μg of protein of INS-1E cells was analyzed per lane on 12% SDS-polyacrylamide gels. Proteins were transferred onto nitrocellulose membrane and subsequently incubated overnight at 4 °C in the presence of goat anti-SIRT4 polyclonal antibody (1:500) raised against human SIRT4 (Abcam, Cambridge, MA). The membrane was then incubated for 2 h with donkey anti-goat IgG antibody (1:5000) conjugated to horseradish peroxidase (Santa Cruz Biotechnology, Inc., Santa Cruz, CA), and the SIRT4 protein was revealed by chemiluminescence (Pierce).

Insulin Secretion Assay—INS-1E cells cultured in 24-well plates were transfected with 250 nM control siRNA or siRNA-SIRT4 and assayed 3 days after for insulin secretion as previously described (20). Prior to the experiments, cells were maintained for 2 h in glucose- and glutamine-free culture medium. The cells were then washed and preincubated further in glucose-free KRBH, supplemented with 0.1% bovine serum albumin as carrier, before the incubation period (30 min at 37 °C) at basal (2.5 mM) and stimulatory (7.5 and 15 mM) glucose concentrations, with the mitochondrial substrate methyl-succinate (5 mM) as well as in the presence 30 mM KCl used as a calcium-raising agent. At the end of the incubation period, supernatants were collected and quantified for absolute insulin secretion, and insulin was extracted from cells using acid-EtOH in order to measure total insulin content. Insulin levels were determined by radioimmunoassay using rat insulin as standard, and secretion was expressed according to cellular protein concentrations.

Cellular ATP Monitoring—ATP levels were monitored in INS-1E cells expressing the ATP-sensitive bioluminescent probe luciferase following infection with the specific viral construct. Briefly, cells were transduced with AdCA-cLuc (driving the expression of cytosolic luciferase) and used 20 h later for experiments. Cells were washed with 1 ml of KRBH and incubated for 30 min at 37 °C at 2.5 mM glucose. Then KRBH containing 100 μM luciferin was added, and the luminescence was monitored in the plate reader luminometer (Fluostar Optima) (20).

Statistical Analysis—Where applicable, the results were expressed as means ± S.D. Differences between groups were analyzed by Student's *t* test for unpaired data, and significance was assessed by a *p* value of less than 0.05.

RESULTS

SIRT4 Is a Mitochondrial Protein—To study the subcellular localization of human SIRT4, HeLa cells were transiently transfected with a plasmid encoding SIRT4-FLAG. Immunofluorescence analysis of the transfected cells by confocal microscopy showed that SIRT4-FLAG was exclusively localized in discrete rod-shaped structures in the cytosol that were reminiscent of mitochondria (Fig. 1*A*). The colocalization of this fluorescence with MitoTracker Red, a dye that preferentially accumulates in mitochondria, confirmed the mitochondrial localization of SIRT4 in the HeLa cells (Fig. 1*A*).

To further verify the subcellular localization of SIRT4, HEK293T cells expressing the SIRT4-FLAG protein were fractionated by differential centrifugation in a mitochondria-enriched fraction (HM), a fraction containing microsomes (LM), and into a cytosolic protein fraction (S100). Immunoblot analysis revealed that SIRT4 was exclusively localized in the HM fraction (Fig. 1*B*). The purity of these fractions was confirmed by probing for the mitochondrial marker cytochrome *c* and the cytosolic marker Hsp90.

To determine if endogenous SIRT4 is also localized to the mitochondria, a rabbit polyclonal antiserum was generated against a peptide corresponding to the last 15 amino acids of human SIRT4. The antiserum reacted strongly with a 29-kDa protein in the mitochondria-enriched fraction of HEK293T cells (Fig. 1*C*).

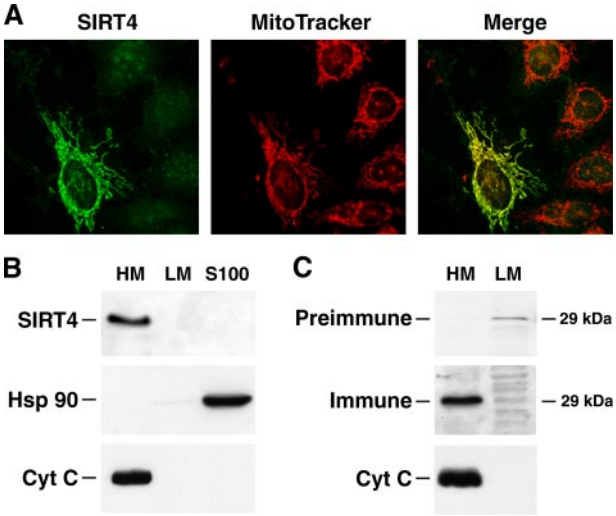

FIGURE 1. **Subcellular localization of SIRT4.** *A*, HeLa cells were grown on coverslips and transfected with SIRT4-FLAG. Transfected cells were stained with Mitotracker Red, permeabilized, incubated with mouse monoclonal anti-FLAG antibody and Cy2-conjugated anti-mouse antibody, and visualized with confocal laser-scanning microscopy. *B*, HEK293T cells transfected with SIRT4-FLAG were homogenized and subjected to differential centrifugation to separate the HM, LM, and cytosolic fractions. Equal amounts of protein from each fraction were analyzed by SDS-PAGE and Western blotting with antibodies against Hsp90 (cytosol) and cytochrome *c* (mitochondria). Mouse monoclonal anti-FLAG antibody was used to detect SIRT4-FLAG. *C*, HEK293T cells were homogenized and subjected to differential centrifugation to separate the subcellular fractions. Equal amounts of protein from HM and LM fractions were analyzed by SDS-PAGE and by Western blotting with preimmune serum or antiserum against SIRT4 or an antibody against cytochrome *c*.

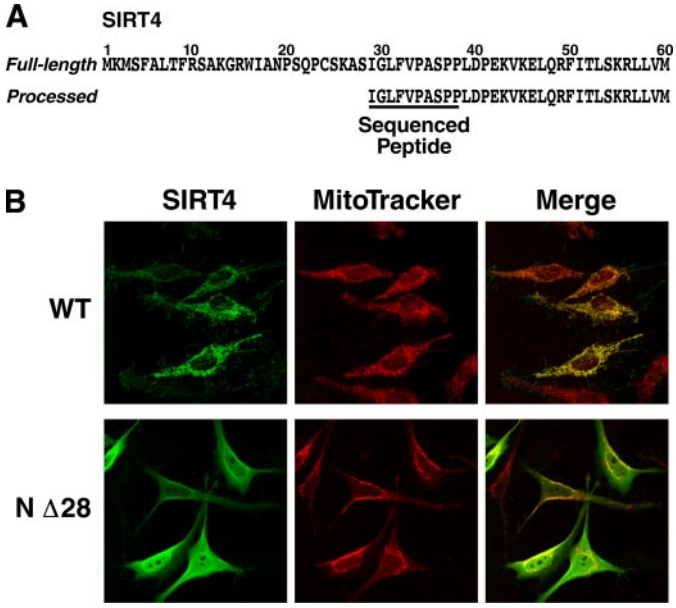

FIGURE 2. **SIRT4 is proteolytically processed in the mitochondria.** *A*, HEK293T cells were transfected with SIRT4-FLAG. The mitochondria were isolated, and SIRT4-FLAG was immunoprecipitated with anti-FLAG M2-agarose affinity gel. The immunoprecipitated protein was subjected to SDS-PAGE, transferred onto a polyvinylidene difluoride membrane, and subjected to NH_2-terminal sequencing by Edman degradation. The sequence obtained (IGLFVPASPP) is aligned with the predicted sequence of full-length SIRT4. *B*, HeLa cells were grown on coverslips and transfected with SIRT4-FLAG or an NH_2-terminal deletion mutant lacking the first 28 amino acids (NΔ28). Cells were stained with Mitotracker Red, permeabilized, and incubated with mouse monoclonal anti-FLAG antibody, and anti-mouse Cy2 antibody. Cells were analyzed using confocal laser-scanning microscopy. *WT*, wild type.

SIRT4 Is Proteolytically Processed at Its NH_2 Terminus—The human SIRT4 cDNA encodes a protein with a predicted molecular mass of 35 kDa. However, both endogenous and FLAG-tagged SIRT4 detected in the mitochondria migrated on SDS-polyacrylamide gels with an apparent molecular mass of 29 kDa. This observation is consistent with the possibility that SIRT4 is proteolytically processed, as observed for many mitochondrial proteins. The polyclonal antiserum used to detect endogenous SIRT4 was raised against its COOH terminus and recognized the shorter form of SIRT4, suggesting that processing occurs at the NH_2 terminus. To check for this possibility, SIRT4-FLAG (FLAG epitope at the COOH terminus) was overexpressed in HEK293T cells, immunoprecipitated from mitochondrial extracts, and subjected to NH_2-terminal sequencing by Edman degradation. This analysis revealed that the first 28 amino acids of SIRT4 are absent from the mature form of the protein located in the mitochondria (Fig. 2*A*).

A deletion mutant of SIRT4 lacking the first 28 residues (NΔ28) showed diffuse fluorescence after transient overexpression (Fig. 2*B*). This observation indicated that the NH_2-terminal 28 residues of SIRT4 are required for correct targeting of SIRT4 to the mitochondria and that the NH_2-terminal processing of SIRT4 most likely occurs after the protein reaches the mitochondria. We also tested a series of NH_2-terminal deletion mutants of SIRT4 for mitochondrial localization and observed that deletion of the first 10 amino acids of SIRT4 abrogates mitochondrial targeting (data not shown).

SIRT4 Resides in the Mitochondrial Matrix—Four distinct subcompartments can be distinguished within mitochondria: the outer membrane, the inner membrane, the intermembrane space, and the matrix. To determine the submitochondrial localization of SIRT4, partially purified mitochondria were treated with proteinase K to remove all nonmitochondrial proteins and proteins associated with the outer membrane. SIRT4 was protease-insensitive under these conditions, indicating that it is not associated with the outer membrane and is present within the mitochondria (Fig. 3*A*). Three mitochondrial markers, Hsp60, CoxIV, and cytochrome *c*, were also resistant to the protease treatment under these conditions (Fig. 3*A*). Permeabilization of mitochondria with Triton X-100 rendered all proteins susceptible to protease digestion, as expected (Fig. 3*A*). Mitoplasts, which represent mitochondria stripped of their outer membrane and intermembrane compartment, were prepared by resuspension of mitochondria in hypotonic buffer to disrupt the outer membrane. Digestion of mitoplasts with proteinase K caused degradation of cytochrome *c*, an intermembrane protein, whereas the matrix protein Hsp60 was insensitive, as predicted (Fig. 3*A*). SIRT4 was resistant to proteinase K in mitoplasts (Fig. 3*A*), indicating that SIRT4 might be integrated in the inner membrane, peripherally attached to the inner side of the inner membrane, or residing as a soluble protein in the mitochondrial matrix.

To distinguish between these possibilities, alkaline sodium carbonate extraction of the mitochondria was carried out. In this procedure, soluble proteins are extracted and separated from integral membrane proteins after centrifugation. After this treatment, the soluble mitochondrial matrix marker Hsp70 was found in the supernatant, whereas the integral inner mem-

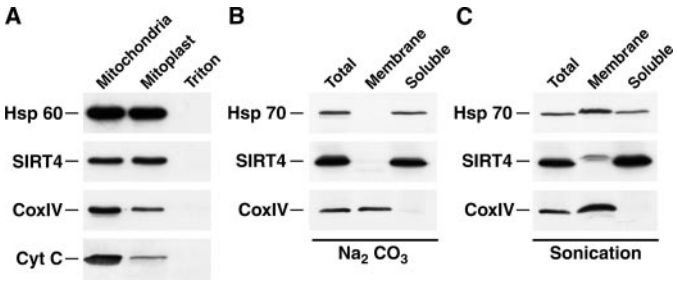

FIGURE 3. **SIRT4 resides in the mitochondrial matrix.** *A*, HEK293T cells were transfected to overexpress SIRT4-FLAG. Mitochondria were isolated and maintained under isotonic conditions, diluted with hypotonic buffer to create mitoplasts, or lysed in Triton X-100. Proteinase K was added to these preparations to digest accessible proteins. The resulting digestion was analyzed by Western blotting with antibodies against intermembrane space protein cytochrome *c* (*Cyt C*), inner membrane protein CoxIV, and matrix protein Hsp60. Anti-FLAG M2 antibodies were used to detect SIRT4-FLAG. *B*, mitochondria were isolated from HEK293T cells transfected with SIRT4-FLAG and resuspended in SDS sample buffer (*Total*) or in freshly prepared alkaline sodium carbonate buffer. The extract was centrifuged at 100,000 × *g*, and mitochondrial membranes (*Membrane*) were resuspended in SDS sample buffer. The supernatant containing the soluble and peripheral membrane proteins (*Soluble*) was precipitated with tricarboxylic acid before SDS-PAGE. Samples were analyzed by Western blotting with antibodies against the soluble matrix protein mitochondrial Hsp70 and CoxIV. SIRT4 was detected with monoclonal anti-FLAG M2 antibodies. *C*, mitochondria were isolated from cells expressing SIRT4-FLAG, resuspended in Tris buffer, and sonicated. Membranes were separated from the soluble proteins by centrifugation at 100,000 × *g*.

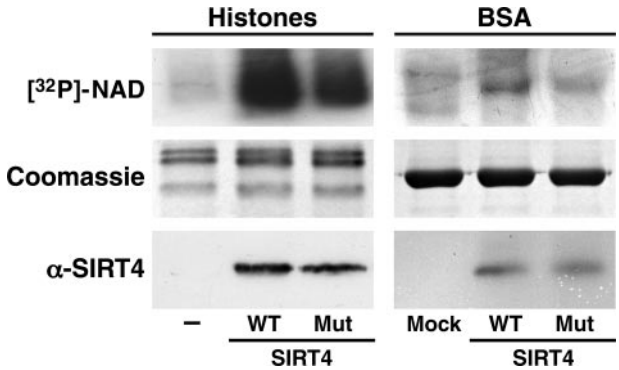

FIGURE 4. **Immunoprecipitated SIRT4 is associated with ADP-ribosyltransferase activity.** Lysates from control cells or cells transfected with a SIRT4-FLAG vector or the mutant SIRT4-H161Y-FLAG were immunoprecipitated and incubated either with total histone proteins or with BSA in the presence of [^{32}P]NAD for 1 h at 37 °C. The reaction mix was separated by SDS-PAGE, stained by Coomassie (*Coomassie*), and exposed to film for autoradiography ([^{32}P]NAD). An aliquot was analyzed by Western blotting using an antiserum specific for FLAG (α-SIRT4). *WT*, wild type.

brane marker, CoxIV, was recovered in the membrane pellet (Fig. 3*B*). SIRT4 was found in the supernatant, indicating that it resides in the mitochondrial matrix, either as a soluble protein or peripherally associated with the inner face of the inner mitochondrial membrane (Fig. 3*B*).

To further confirm these results, mitochondria were sonicated in a hypotonic solution. Membrane-associated proteins were separated from soluble proteins by centrifugation. Immunoblot analysis of these fractions revealed that SIRT4 was predominantly present as a soluble protein (Fig. 3*C*). These results indicate that SIRT4 is a soluble mitochondrial matrix protein.

Immunoprecipitated SIRT4 Is Associated with ADP-ribosyltransferase Activity—We have previously reported that SIRT4 exhibited no histone deacetylase activity on a histone peptide (13). Multiple additional attempts were made to detect a protein deacetylase activity associated with SIRT4. These included the expression and purification of SIRT4 in *Escherichia coli* and the use of other potential substrates, including a modified acetyl-lysine substrate (Fluor de Lys). These experiments were uniformly negative, and no protein deacetylase activity could be identified in association with SIRT4 (data not shown). Another mammalian sirtuin, SIRT6, also shows no detectable protein deacetylase activity (13) and was recently demonstrated to function as an ADP-ribosyltransferase (18). To test the possibility that SIRT4 might also exhibit ADP-ribosyltransferase activity, we immunoprecipitated SIRT4-FLAG or the mutant SIRT4-H161Y from HEK293 cells after overexpression and incubated the immunoprecipitated material either with total histone proteins or with BSA in the presence of [^{32}P]NAD. This experiment indicated that immunoprecipitated SIRT4 catalyzed the ADP-ribosylation of histone proteins and, to a lesser degree, of BSA using NAD as a donor (Fig. 4). ADP-ribosylation of histones and BSA was reduced when the SIRT4 mutant H161Y was used in these experiments (Fig. 4).

Identification of SIRT4-associated Proteins by Mass Spectrometry—To identify SIRT4-associated proteins, we first established a SIRT4-FLAG-overexpressing stable cell line and a control cell line containing the empty vector. These cells were harvested and lysed, and SIRT4-FLAG was immunoprecipitated. The immunoprecipitated material was washed at high stringency (300 mM NaCl) to remove nonspecifically associated proteins and resuspended in SDS-lysis buffer. SDS-PAGE analysis revealed three prominent bands of 110, 50, and 35 kDa, respectively. These bands were specifically associated with SIRT4 and not immunoprecipitated from the control cell line (data not shown). These bands were excised from the gel and subjected to mass spectrometry analysis. The 110 kDa band was identified as insulin-degrading enzyme (IDE). Thirty-six unique peptides were identified spanning the complete sequence of IDE with a coverage of 36% of the reported IDE sequence (see supplemental materials). IDE is a thiol-dependent metalloprotease that regulates amyloid β peptide levels and insulin levels *in vivo* (23–25). Translation of IDE at an in-frame initiation codon 123 nucleotides upstream of the canonical translation start site results in the addition of a 41-amino acid NH_2-terminal mitochondrial targeting sequence and leads to the mitochondrial localization of a fraction of the total cellular IDE (26). The 50 kDa band was a complex mixture of proteins that did not yield conclusive results (data not shown). The 35 kDa band contained ANT2 (ATP/ADP translocase 2), and most likely also ANT3. ANT2 and ANT3 show 92.9% identity. Nine and eight peptides were matched to sequences of ANT2 and ANT3, resulting in 34 and 26% sequence coverage, respectively (supplemental materials). ATP/ADP translocase 2 and 3 are inner mitochondrial membrane proteins that catalyze the exchange of ATP generated in the mitochondria by ATP synthase against ADP produced in the cytosol (27).

SIRT4 Co-immunoprecipitates with IDE and ANT2—To confirm the interaction between SIRT4 and IDE or ANT2, we conducted immunoprecipitation experiments. Lysates from HEK293 cells stably expressing either SIRT4-FLAG or SIRT5-FLAG were immunoprecipitated with an antiserum against FLAG. The immunoprecipitated material was analyzed by Western blotting using antisera specific for endogenous SIRT3,

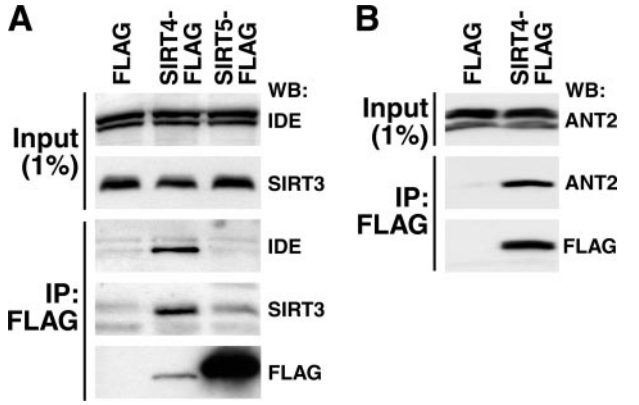

FIGURE 5. **SIRT4 co-immunoprecipitates with endogenous IDE and ANT2.** *A*, HEK293 cells stably expressing SIRT4-FLAG, SIRT5-FLAG, or the empty FLAG control vector were immunoprecipitated with anti-FLAG antibodies. The immunoprecipitates (*IP*) were analyzed by Western blotting (*WB*) with antibodies recognizing endogenous IDE or SIRT3. Endogenous IDE and SIRT3 were only immunoprecipitated in the presence of SIRT4-FLAG. Western blotting analysis demonstrated the presence of equal amounts of IDE or SIRT3 in the cell lysates used for immunoprecipitation (*Input*). *B*, SIRT4 interacts with ANT2. HEK293 cells stably expressing SIRT4-FLAG or the empty FLAG-control vector were immunoprecipitated using anti-FLAG antibodies. Immunoprecipitates were analyzed by Western blotting using anti-ANT2 antibodies. ANT2 was only detectable in the presence of SIRT4-FLAG. Analysis of the input material (*Input*) demonstrated that equal amounts of ANT2 were expressed in the lysates used for immunoprecipitation.

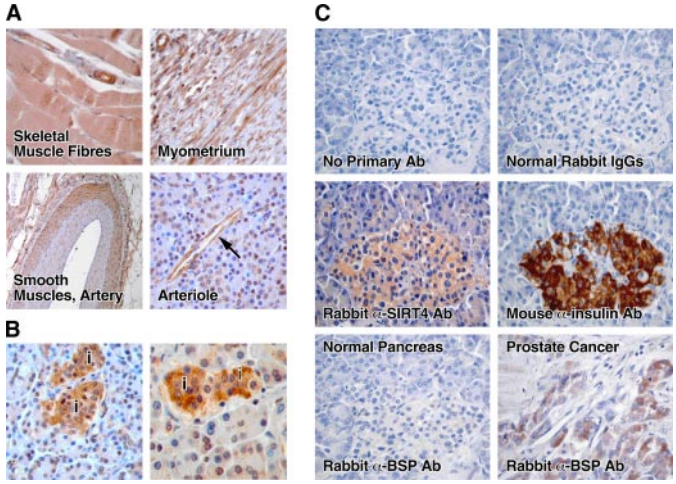

FIGURE 6. **SIRT4 is expressed in skeletal and smooth muscle cells and in pancreatic insulin-producing β cells.** Expression of SIRT4 was examined using immunohistochemistry in several human tissues. *A*, skeletal muscle, myometrium, and smooth muscles of arteries and arterioles in pancreas; *B*, islet of Langerhans (*i*) in normal pancreatic tissue. *C*, adjacent slices of human pancreatic tissue were stained either with no primary antibody, with normal rabbit IgGs, with a rabbit anti-SIRT4 antibody, with a mouse anti-insulin antibody, or with a rabbit anti-bone sialoprotein (*BSP*) antibody. As a positive control, the same rabbit anti-bone sialoprotein antibody was used against a section of poorly differentiated human prostate cancer.

IDE, or ANT2. We observed that endogenous IDE immunoprecipitated with SIRT4-FLAG. Surprisingly, endogenous SIRT3, another matrix mitochondrial sirtuin (14), also co-immunoprecipitated with SIRT4. These interactions were specific, since SIRT5-FLAG did not co-immunoprecipitate with either IDE or SIRT3 under the same conditions, despite being expressed at a much higher level in these cells (Fig. 5*A*). Western blotting analysis demonstrated the presence of equal amounts of IDE or SIRT3 in the cell lysates used for immunoprecipitation (Fig. 5*A*). Using the same experimental approach, we also found that endogenous ANT2 co-immmunoprecipitated with SIRT4-FLAG (Fig. 5*B*). Analysis of the input material (*Input*) demonstrated that equal amounts of ANT2 were expressed in the lysates used for immunoprecipitation (Fig. 5*B*).

SIRT4 Is Expressed in a Variety of Organs and Cell Types, Including the β Cells of the Pancreatic Islets of Langerhans—SIRT4 transcripts have been detected in normal human tissues by Northern blot, including muscle, kidney, testis, and liver (28). We used immunohistochemistry and a specific antiserum against SIRT4 to detect SIRT4 protein levels in different human tissues. We observed significant SIRT4 expression in various cell types, including vascular smooth muscle cells and striated muscle fibers, with a predominant cytoplasmic localization (Fig. 6*A*). A weak but detectable amount of SIRT4 expression was observed in pancreatic acini, whereas strong anti-SIRT4 immunoreactivity was detected in islets of Langerhans (Fig. 6*B*). Staining with an anti-insulin antibody on companion sections indicated that SIRT4 is expressed by insulin-producing β cells within the endocrine pancreas (Fig. 6*C*). The specificity of this staining was verified by several controls, including the following: no primary antibody on normal human pancreas, normal rabbit IgGs on normal human pancreas, rabbit anti-bone sialoprotein antibody on normal human pancreas, and rabbit anti-bone sialoprotein antibody on a case of poorly differentiated human prostate cancer (Fig. 6*C*).

Knockdown of SIRT4 via siRNA Enhances Insulin Secretion in β Cells—The expression of SIRT4 in β cells in the pancreas and its interaction with IDE and ANT2/3, two proteins that could modulate insulin secretion, suggested that SIRT4 might regulate insulin secretion. To test this possibility, SIRT4 was depleted from an insulin-producing cell line (INS-1E) using siRNA, and insulin secretion in response to glucose was measured. Knockdown of SIRT4 expression by siRNA led to a 5-fold decrease in SIRT4 mRNA in INS-1E cells (Fig. 7*A*) and to a more than 2-fold decrease at the protein level, as detected by Western blotting (Fig. 7*B*). Insulin secretion in the supernatant of these cells was measured under low glucose (2.5 mM), high glucose (15 mM), and 30 mM KCl. In INS-1E cells treated with the control siRNA, insulin secretion was stimulated 5.0-fold by 15 mM glucose in comparison with 2.5 mM glucose. The calcium-raising agent KCl (30 mM) induced a 2.2-fold secretory response. In SIRT4-depleted cells, no significant change in basal release or in the response to KCl response was noted in comparison with cells treated with the control siRNA. In contrast, glucose-stimulated insulin secretion was potentiated by 45% when SIRT4 was knocked down (Fig. 7*B*). Total cellular insulin contents were not significantly changed by knocking down SIRT4 (14.2 ± 5.5 *versus* 16.2 ± 5.7 ng of insulin/mg of protein).

SIRT4 knockdown did not modify basal insulin secretion. In contrast, at high glucose concentrations, insulin secretion was markedly (40%) increased in cells depleted of SIRT4 (Fig. 7*C*). Importantly, when insulin secretion was stimulated with a non-nutrient secretagogue (KCl), bypassing mitochondrial activation, no significant change in insulin secretion was observed in SIRT4-depleted INS-1E cells (Fig. 7*C*).

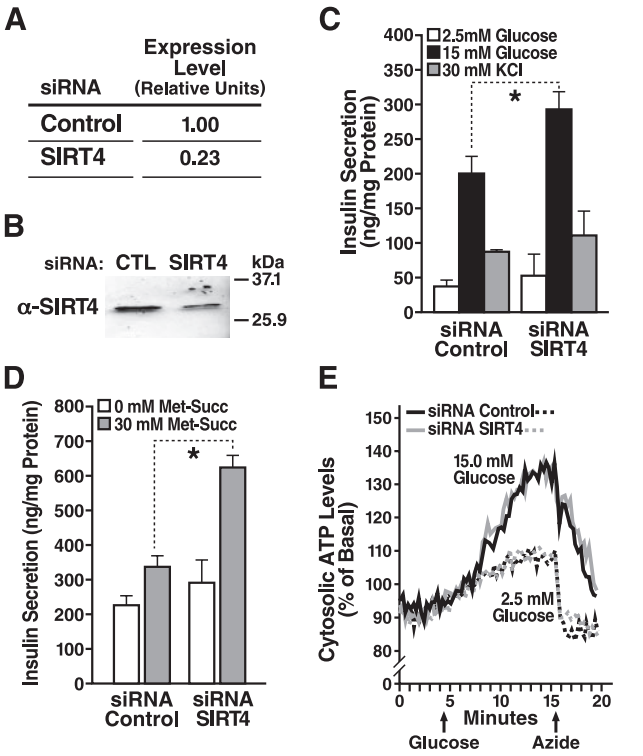

FIGURE 7. **Increased insulin secretion after knockdown of SIRT4 in insulin-producing INS-1E cells.** Control siRNA or siRNA against SIRT4 was transfected into INS-1E cells, and depletion of SIRT4 was measured at the mRNA level by Taqman analysis (*A*) and at the protein level by Western blot analysis (*B*) (identical amounts of total protein are loaded in each *lane*). *C*, insulin secretion was measured after transfection of control siRNA (Dharmacon *SMART*pool™ control) or siRNA against SIRT4 (Dharmacon *SMART*pool™) at low (2.5 mM) and high (15 mM) glucose and after stimulation with the nonnutrient secretagogue, KCl. Results are means ± S.D. ($n = 3$) of one representative of three independent experiments. *, $p < 0.05$ *versus* glucose-matched control. *D*, insulin secretion was measured after transfection of control siRNA (Dharmacon *SMART*pool™ control) or siRNA against SIRT4 (Dharmacon *SMART*pool™) with or without 5 mM methyl-succinate (*Met-suc*). Results are means ± S.D. ($n = 3$) of one representative of three independent experiments. *, $p < 0.05$. *E*, ATP levels were monitored in INS-1E cells (treated with SIRT4 siRNA or control siRNA) expressing the ATP-sensitive bioluminescent probe luciferase (via adenoviral vector). Cells were incubated for 30 min in 2.5 mM glucose, followed by the addition of 100 μM luciferin and measurement of luminescence. Cells were subsequently treated either with high glucose (15 mM) or azide. Results are presented as relative luminescence (percentage of basal) as a function of time (in min).

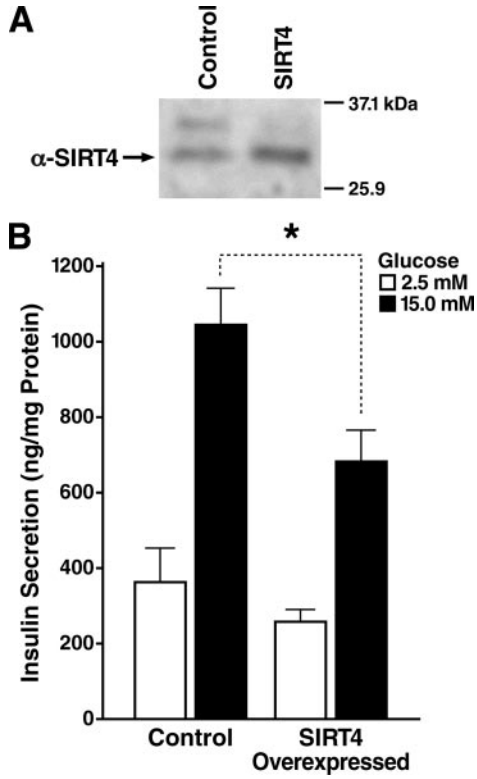

FIGURE 8. **Overexpression of SIRT4 suppresses insulin secretion.** *A*, an expression vector for SIRT4-FLAG or the empty vector control was transfected into INS-1E cells, and total SIRT4 expression was measured with an antiserum specific for SIRT4 by Western blot analysis (identical amounts of total protein are loaded in each *lane*). *B*, insulin secretion was measured in cells transfected with an empty control vector or with the SIRT4-FLAG expression vector at low (2.5 mM) and high (15 mM) glucose. Results are means ± S.D. ($n = 3$) of one representative of three independent experiments. *, $p < 0.05$ *versus* glucose-matched control.

In agreement with the proposed role of SIRT4 in insulin secretion via its activity in mitochondria, we also observed a potentiation of insulin secretion after treatment of INS-1E cells with a fuel that is directly metabolized by mitochondria, methyl-succinate (29). This experiment shows that methyl-succinate-evoked insulin secretion was significantly potentiated when SIRT4 was down-regulated via siRNA (Fig. 7*D*).

Based on these observations, SIRT4 could act at the level of stimulus-secretion coupling, possibly by modifying cytoplasmic ATP concentrations. To test this hypothesis, we measured cytoplasmic ATP concentrations in INS-1E β-cells in which SIRT4 has been knocked down via siRNA. No difference in glucose-induced ATP generation was noted when comparing cells transfected with a control siRNA with those transfected with an a SIRT4-specific siRNA (Fig. 7*E*). However, this experiment does not exclude the possibility that local changes in ATP concentrations occur at the microdomain level (*i.e.* at a point of close proximity between the mitochondria and K-ATP channels at the plasma membrane).

SIRT4 Overexpression Suppresses Insulin Secretion in β Cells—To further examine the role of SIRT4 in insulin secretion, we transfected INS-1E cells with an expression vector for SIRT4. Western blot analysis measuring total SIRT4 content showed a doubling of SIRT4 expression after transfection of the SIRT4 expression vector in comparison with the empty control vector (Fig. 8*A*). Measurement of insulin secretion under the same conditions showed that overexpression of SIRT4 was associated with a significant inhibition of insulin secretion in response to 15 mM glucose (Fig. 8*B*). These observations further support the role of SIRT4 in controlling insulin secretion in response to glucose.

DISCUSSION

Protein trafficking in eukaryotic cells is a complex process coordinated by a variety of signal motifs. Proteins destined for the various subcellular organelles, such as nucleus, mitochondria, and endoplasmic reticulum, all travel distinct pathways. Although mitochondria have their own genome, 99% of all mitochondrial proteins are encoded by nuclear genes and are synthesized as precursors on cytosolic ribosomes, after which they are imported into the organelle (30). This study demonstrates that SIRT4 is localized in the mitochondria of mamma-

lian cells. The subcellular localization of SIRT4 was determined both by confocal microscopy and cell fractionation studies, using an epitope-tagged SIRT4 and/or examining the endogenous protein. Using a combination of protease protection assays and alkaline sodium carbonate extraction of mitochondria, we observed that SIRT4 resides in the mitochondrial matrix as a soluble protein.

Mitochondrial targeting sequences are classified into two major categories (30). The more common class contains mitochondrial precursor proteins with cleavable, NH_2-terminal extensions or presequences of 20–50 amino acids that are rich in positively charged, hydrophobic, and hydroxylated residues and have a potential to form an amphiphilic α-helix with one hydrophobic face and one positively charged face (31, 32). The NH_2-terminal presequences function as targeting signals that interact with the mitochondrial import receptors and direct the preproteins across both the outer and inner membranes (33). The second class has noncleavable sequences that are usually distributed throughout the length of the proteins and are generally not rich in basic amino acids (30).

Our observations indicate that SIRT4 behaves as a typical mitochondrial matrix protein. Sequencing of the SIRT4 protein present in the mitochondrial matrix indicates that it is lacking the first 28 amino acids predicted by the cDNA sequence. A similar cleavage of presequences by mitochondrial proteases is observed for most matrix proteins after import into the mitochondria (34). SIRT4 is synthesized as a precursor protein with a positively charged 28-amino acid leader peptide that is required for targeting to the mitochondria. Immunofluorescence microscopy of a SIRT4 deletion mutant lacking the first 10 or 28 NH_2-terminal residues showed that the mutant proteins are distributed throughout the cell and are not specifically targeted to the mitochondria.

Secondary structure prediction of SIRT4 also identified residues 45–56 as having a high potential to form an amphiphilic α-helix. Mutational analysis of this amphiphilic helix revealed that mitochondrial targeting of SIRT4 is disrupted when the amphiphilicity of this helix is eliminated by replacing basic residues with glutamines.[4] Therefore, the amphiphilic helix between residues 45 and 56 of SIRT4 contributes to mitochondrial targeting of SIRT4 and is distinct from the leader peptide.

In agreement with these observations, Michishita *et al.* (35) also reported that human SIRT4 and SIRT5 fused to GFP colocalize with the mitochondrial marker MitoFluor.

Despite numerous attempts using a variety of expression systems and substrates, we have not detected any deacetylase activity associated with the SIRT4 protein. Unexpectedly, we have observed that immunoprecipitated SIRT4 is associated with a strong and reproducible ADP-ribosyltransferase activity. A similar observation was recently made for SIRT6 (18). However, SIRT6 catalytic activity appeared to be exclusively intramolecular, with individual molecules of SIRT6 directing their own modification. This is in contrast to SIRT4, which catalyzes the modification of both histones and BSA *in vitro*. Our observations are therefore consistent with the possibility that SIRT4 mediates the ADP-ribosylation of select mitochondrial proteins. Several proteins have been reported to be ribosylated in mitochondria, including the adenine nucleotide transporter (36, 37) and glutamate dehydrogenase (38). We have observed that glutamate dehydrogenase coimmunoprecipitates with SIRT4 but were unable to detect its presence in SIRT4-associated proteins by mass spectrometry (data not shown). There are no reports on the ADP-ribosylation of IDE, and its role in the mitochondrion is at present unclear. Future experiments will explore the possible role of SIRT4 as a mitochondrial ADP-ribosyltransferase targeting IDE and ANT2/3.

Insulin secretion by pancreatic β islet cells is tightly regulated by glucose levels (for a review, see Ref. 39). In the β cell, glucose is rapidly metabolized via glycolysis for entry into the mitochondrial tricarboxylic acid cycle (40). The mitochondrial inner membrane protein ATP/ADP translocase exchanges mitochondrial ATP, produced by oxidative phosphorylation, for cytosolic ADP. This leads to an increase in cytosolic ATP/ADP ratio, followed by closure of ATP-sensitive K^+ channels and depolarization of the plasma membrane (41). Voltage-dependent calcium channels respond to this membrane depolarization by increasing cytosolic calcium, which then triggers the fusion of insulin-containing secretory vesicles to the plasma membrane to cause insulin exocytosis (42). Insulin secretion is therefore tightly linked to glucose metabolism via its ability to produce ATP in the mitochondria.

IDE is a widely expressed zinc metalloprotease that regulates both cerebral amyloid β peptide levels and plasma insulin levels *in vivo* (23, 24). Partial loss-of-function mutations of IDE that induce diabetes also impair degradation of amyloid β protein (43). The IDE region of chromosome 10q has been linked to late onset Alzheimer disease and diabetes mellitus (44). In the inbred rat model of Type II diabetes mellitus, the Goto-Kakizaki rat, two missense mutations, $His^{18} \rightarrow$ Arg and $Ala^{890} \rightarrow$ Val, decrease the ability of IDE to degrade insulin and hence confer the diabetic phenotype (45). It is interesting to note that the His^{18} residue is contained within the mitochondrial targeting sequence of IDE, suggesting that the mitochondrial form of IDE is involved in the diabetic phenotype. The nature of the mitochondrial target(s) of IDE is at present unclear.

We report here that SIRT4 is highly expressed in islet β cells, interacts with the ANT2/3 subunit of the ATP/ADP translocase and the IDE protease, and negatively regulates insulin secretion. A possible model accounting for our observations is that SIRT4 modifies ANT2/3, and possibly IDE, by ADP-ribosylation and changes their activity as an ATP/ATP translocase and as a protease. This in turn would change the levels of insulin secretion in response to glucose.

The role of sirtuins in the control of insulin secretion and metabolism is growing increasingly complex (reviewed in Refs. 1–3 and 46). A possible genetic link between Sir2 and the insulin/IGF-1 pathway has been reported in *Caenorhabditis elegans* (47). Two recent reports have reported on the existence of a similar link in mammals (48, 49). Both studies indicated that SIRT1 positively regulates insulin secretion in pancreatic β cells, in part by regulating the expression of the mitochondrial uncoupling protein 2, another protein that may modulate ATP provision. Our new observations bring another level of com-

[4] N. Ahuja, B. Schwer, S. Carobbio, D. Waltregny, B. J. North, V. Castronovo, P. Maechler, and E. Verdin, unpublished observations.

plexity to this equation by identifying a sirtuin, SIRT4, as a protein that negatively regulates insulin secretion. Haigis *et al.* (50) also reported that SIRT4 is a mitochondrial protein and down-regulates insulin secretion. They identified glutamate dehydrogenase as a target for SIRT4 activity and showed that SIRT4 opposes the effects of calorie restriction in pancreatic β cells (50). Our results are complementary to these observations, further identify two additional targets for SIRT4 (IDE and ANT), and further support the role of SIRT4 in the control of insulin secretion in pancreatic β cells. Future experiments in mice lacking either SIRT1 or SIRT4 will be important to ascertain in a comprehensive manner the role of sirtuins in insulin secretion and energy metabolism.

Acknowledgments—We thank John Carroll and Jack Hull for graphics and Amanda Bradford for manuscript preparation. We thank Dr. Steven C. Hall and Dr. H. Ewa Witkowska from the University of California, San Francisco, Biomolecular Resource Center Mass Spectrometry facility. We thank Dr. Laurence de Leval (Department of Pathology, University of Liege) for providing the normal pancreas tissue samples used in the immunohistochemistry experiments and Dr. Douglas Wallace (University of California, Irvine) for providing the ANT2 antiserum.

REFERENCES

1. North, B. J., and Verdin, E. (2004) *Genome Biol.* **5,** 224
2. Denu, J. M. (2005) *Curr. Opin. Chem. Biol.* **9,** 431–440
3. Guarente, L. (2000) *Genes Dev.* **14,** 1021–1026
4. Frye, R. A. (1999) *Biochem. Biophys. Res. Commun.* **260,** 273–279
5. Frye, R. A. (2000) *Biochem. Biophys. Res. Commun.* **273,** 793–798
6. Fulco, M., Schiltz, R. L., Iezzi, S., King, M. T., Zhao, P., Kashiwaya, Y., Hoffman, E., Veech, R. L., and Sartorelli, V. (2003) *Mol. Cell* **12,** 51–62
7. Brunet, A., Sweeney, L. B., Sturgill, J. F., Chua, K. F., Greer, P. L., Lin, Y., Tran, H., Ross, S. E., Mostoslavsky, R., Cohen, H. Y., Hu, L. S., Cheng, H. L., Jedrychowski, M. P., Gygi, S. P., Sinclair, D. A., Alt, F. W., and Greenberg, M. E. (2004) *Science* **303,** 2011–2015
8. Vaziri, H., Dessain, S. K., Ng Eaton, E., Imai, S. I., Frye, R. A., Pandita, T. K., Guarente, L., and Weinberg, R. A. (2001) *Cell* **107,** 149–159
9. Luo, J., Nikolaev, A. Y., Imai, S., Chen, D., Su, F., Shiloh, A., Guarente, L., and Gu, W. (2001) *Cell* **107,** 137–148
10. Yeung, F., Hoberg, J. E., Ramsey, C. S., Keller, M. D., Jones, D. R., Frye, R. A., and Mayo, M. W. (2004) *EMBO J.* **23,** 2369–2380
11. Langley, E., Pearson, M., Faretta, M., Bauer, U. M., Frye, R. A., Minucci, S., Pelicci, P. G., and Kouzarides, T. (2002) *EMBO J.* **21,** 2383–2396
12. Motta, M. C., Divecha, N., Lemieux, M., Kamel, C., Chen, D., Gu, W., Bultsma, Y., McBurney, M., and Guarente, L. (2004) *Cell* **116,** 551–563
13. North, B. J., Marshall, B. L., Borra, M. T., Denu, J. M., and Verdin, E. (2003) *Mol. Cell* **11,** 437–444
14. Schwer, B., North, B. J., Frye, R. A., Ott, M., and Verdin, E. (2002) *J. Cell Biol.* **158,** 647–657
15. Onyango, P., Celic, I., McCaffery, J. M., Boeke, J. D., and Feinberg, A. P. (2002) *Proc. Natl. Acad. Sci. U. S. A.* **99,** 13653–13658
16. Min, J., Landry, J., Sternglanz, R., and Xu, R. M. (2001) *Cell* **105,** 269–279
17. Avalos, J. L., Celic, I., Muhammad, S., Cosgrove, M. S., Boeke, J. D., and Wolberger, C. (2002) *Mol. Cell* **10,** 523–535
18. Liszt, G., Ford, E., Kurtev, M., and Guarente, L. (2005) *J. Biol. Chem.* **280,** 21313–21320
19. Garcia-Salcedo, J. A., Gijon, P., Nolan, D. P., Tebabi, P., and Pays, E. (2003) *EMBO J.* **22,** 5851–5862
20. Merglen, A., Theander, S., Rubi, B., Chaffard, G., Wollheim, C. B., and Maechler, P. (2004) *Endocrinology* **145,** 667–678
21. Asfari, M., Janjic, D., Meda, P., Li, G., Halban, P. A., and Wollheim, C. B. (1992) *Endocrinology* **130,** 167–178
22. Graham, B. H., Waymire, K. G., Cottrell, B., Trounce, I. A., MacGregor, G. R., and Wallace, D. C. (1997) *Nat. Genet.* **16,** 226–234
23. Farris, W., Mansourian, S., Chang, Y., Lindsley, L., Eckman, E. A., Frosch, M. P., Eckman, C. B., Tanzi, R. E., Selkoe, D. J., and Guenette, S. (2003) *Proc. Natl. Acad. Sci. U. S. A.* **100,** 4162–4167
24. Miller, B. C., Eckman, E. A., Sambamurti, K., Dobbs, N., Chow, K. M., Eckman, C. B., Hersh, L. B., and Thiele, D. L. (2003) *Proc. Natl. Acad. Sci. U. S. A.* **100,** 6221–6226
25. Kurochkin, I. V., and Goto, S. (1994) *FEBS Lett.* **345,** 33–37
26. Leissring, M. A., Farris, W., Wu, X., Christodoulou, D. C., Haigis, M. C., Guarente, L., and Selkoe, D. J. (2004) *Biochem. J.* **383,** 439–446
27. Pebay-Peyroula, E., and Brandolin, G. (2004) *Curr. Opin. Struct. Biol.* **14,** 420–425
28. Shi, T., Wang, F., Stieren, E., and Tong, Q. (2005) *J. Biol. Chem.* **280,** 13560–13567
29. Kennedy, E. D., Maechler, P., and Wollheim, C. B. (1998) *Diabetes* **47,** 374–380
30. Chacinska, A., Pfanner, N., and Meisinger, C. (2002) *Trends Cell Biol.* **12,** 299–303
31. Pfanner, N. (2000) *Curr. Biol.* **10,** R412–R415
32. Roise, D., Theiler, F., Horvath, S. J., Tomich, J. M., Richards, J. H., Allison, D. S., and Schatz, G. (1988) *EMBO J.* **7,** 649–653
33. Truscott, K. N., Brandner, K., and Pfanner, N. (2003) *Curr. Biol.* **13,** R326–337
34. Luciano, P., and Geli, V. (1996) *Experientia* **52,** 1077–1082
35. Michishita, E., Park, J. Y., Burneskis, J. M., Barrett, J. C., and Horikawa, I. (2005) *Mol. Biol. Cell* **16,** 4623–4635
36. Hardy, D. L., and Mowbray, J. (1992) *Biochem. J.* **283,** 849–854
37. Mowbray, J., and Hardy, D. L. (1996) *FEBS Lett.* **394,** 61–65
38. Herrero-Yraola, A., Bakhit, S. M., Franke, P., Weise, C., Schweiger, M., Jorcke, D., and Ziegler, M. (2001) *EMBO J.* **20,** 2404–2412
39. Maechler, P. (2003) *Curr. Opin. Investig. Drugs* **4,** 1166–1172
40. Newgard, C. B., and McGarry, J. D. (1995) *Annu. Rev. Biochem.* **64,** 689–719
41. Ashcroft, F. M., Proks, P., Smith, P. A., Ammala, C., Bokvist, K., and Rorsman, P. (1994) *J. Cell Biochem.* **55,** (suppl.) 54–65
42. Lang, J. (1999) *Eur. J. Biochem.* **259,** 3–17
43. Farris, W., Mansourian, S., Leissring, M. A., Eckman, E. A., Bertram, L., Eckman, C. B., Tanzi, R. E., and Selkoe, D. J. (2004) *Am. J. Pathol.* **164,** 1425–1434
44. Bertram, L., Blacker, D., Mullin, K., Keeney, D., Jones, J., Basu, S., Yhu, S., McInnis, M. G., Go, R. C., Vekrellis, K., Selkoe, D. J., Saunders, A. J., and Tanzi, R. E. (2000) *Science* **290,** 2302–2303
45. Fakhrai-Rad, H., Nikoshkov, A., Kamel, A., Fernstrom, M., Zierath, J. R., Norgren, S., Luthman, H., and Galli, J. (2000) *Hum. Mol. Genet.* **9,** 2149–2158
46. Blander, G., and Guarente, L. (2004) *Annu. Rev. Biochem.* **73,** 417–435
47. Tissenbaum, H. A., and Guarente, L. (2001) *Nature* **410,** 227–230
48. Bordone, L., Motta, M. C., Picard, F., Robinson, A., Jhala, U. S., Apfeld, J., McDonagh, T., Lemieux, M., McBurney, M., Szilvasi, A., Easlon, E. J., Lin, S. J., and Guarente, L. (2006) *PLoS Biol.* **4,** e31
49. Moynihan, K. A., Grimm, A. A., Plueger, M. M., Bernal-Mizrachi, E., Ford, E., Cras-Meneur, C., Permutt, M. A., and Imai, S. (2005) *Cell Metab.* **2,** 105–117
50. Haigis, M. C., Mostoslavsky, R., Haigis, K. M., Fahie, K., Christodoulou, D. C., Murphy, A. J., Valenzuela, D. M., Yancopoulos, G. D., Karow, M., Blander, G., Wolberger, C., Prolla, T. A., Weindruch, R., Alt, F. W., and Guarente, L. (2006) *Cell* **126,** 941–954